Available online at www.sciencedirect.com
SCIENCE DIRECT®
Journal of Solid State Chemistry 176 (2003) 27–32
JOURNAL OF SOLID STATE CHEMISTRY
http://elsevier.com/locate/jssc

Synthesis, X-ray crystal structure and vibrational spectroscopy of the acidic pyrophosphate $KMg_{0.5}H_2P_2O_7 \cdot H_2O$

M. Harcharras,[a] F. Capitelli,[b,*] A. Ennaciri,[a] K. Brouzi,[a] A.G.G. Moliterni,[b] G. Mattei,[c] and V. Bertolasi[d]

[a] *Laboratory of Spectroscopy, Department of Chemistry, Faculty of Sciences, University Ibn Tofail; B.P.133, 14000 Kenitra, Morocco*
[b] *Dipartimento Geomineralogico, Istituto di Cristallografia (IC-CNR), Via Orabona 4, 70125 Bari, Italy*
[c] *Istituto di Metodologie Inorganiche e dei Plasmi (IMIP-CNR), Area della ricerca di Roma-Montelibretti, Via Salaria Km 29,300, C.P. 10-00016 Monterotondo Stazione Roma, Roma, Italy*
[d] *Dipartimento di Chimica and Centro di Strutturistica Diffrattometrica, Università di Ferrara, Via Borsari 46, 44100 Ferrara, Italy*

Received 4 April 2003; received in revised form 4 June 2003; accepted 6 June 2003

Abstract

The hydrated potassium hemimagnesium dihydrogen pyrophosphate $KMg_{0.5}H_2P_2O_7 \cdot H_2O$ was synthesized. It crystallizes in the triclinic system, space group $P\bar{1}$ (n. 2), $Z = 2$, with the following unit-cell parameters: $a = 6.8565(2)$ Å, $b = 7.3621(3)$ Å, $c = 7.6202(3)$ Å, $\alpha = 81.044(2)^\circ$, $\beta = 72.248(2)^\circ$, $\gamma = 83.314(3)^\circ$, $V = 360.90(2)$ Å^3. The structure was obtained by single-crystal X-ray diffractometry, and a full-matrix least-squares refinement based on F^2 gave a final R index of $=0.0368$ (w$R = 0.0975$), utilizing 1446 observed reflections with $I > 2\sigma(I)$. The crystal packing consists in a three-dimensional network made by layers parallel to *ab* plane of PO_4 double tetrahedra and MgO_6 octahedra, linked by hydrogen bonds, while K atoms form complex coordination within cavities between tetrahedra and octahedra. The dihydro-pyrophosphate anion $(H_2P_2O_7)^{2-}$ shows bent eclipsed conformation and the Mg^{2+} ion lies on inversion center. No coincidences observed between most of infrared and Raman spectral bands confirmed the centrosymmetric structure of the title compound; the vibrational spectra point to a bent POP bridge angle.

Keywords: Pyrophosphate; X-ray single-crystal diffractometry; C_i symmetry; Hydrogen bond; Raman spectroscopy; Infrared spectroscopy

1. Introduction

Inorganic acidic pyrophosphates hold important biochemical roles, such as inhibitors of human immunodeficiency enzymes [1], and as inhibitors of the formation and dissolution of apatite crystals [2]; more, they are used for piezoelectrics, luminescent, ceramic and solid state laser applications [3]. Despite such compounds have been studied for 50 years [4–9], their crystal chemistry lacks systematic structural and vibrational investigations. Among the different classes of such compounds, we quote the dicationic $ABPy \cdot nH_2O$ family, where A is a monovalent cation, B is a mono-, di- or trivalent cation and Py is the $(H_2P_2O_7)^{2-}$ acidic pyrophosphate group. Detailed studies on structure determinations of such compounds are available in crystallography literature on $KAl(H_2P_2O_7)_2$ [10], $K_3Na(H_2P_2O_7)_2$ [11], $K_2Co(H_2P_2O_7)_2 \cdot 2H_2O$ [12], but less common are crystal investigations coupled with vibrational spectroscopy. Recently, we have analyzed the acidic pyrophosphate $Na_4Mg_2(H_2P_2O_7)_4 \cdot 8H_2O$ [13], focusing on the polyhedra coordination and the vibrational study (both Raman and infrared). In the present paper we report the crystal structure of the new dicationic acidic pyrophosphate $KMg_{0.5}H_2P_2O_7 \cdot H_2O$, discussing about the X-ray crystal structure and the results of infrared and Raman vibrational spectroscopy.

2. Experimental

2.1. Synthesis

The aqueous solution of magnesium chloride hexahydrate $MgCl_2 \cdot 6H_2O$ (0.1 M) was added dropwise to the

*Corresponding author. Fax: +39-080-544-2591.
E-mail address: francesco.capitelli@ic.cnr.it (F. Capitelli).

0022-4596/$ - see front matter © 2003 Elsevier Inc. All rights reserved.
doi:10.1016/S0022-4596(03)00339-6

anhydrous tetrapotassium pyrophosphate $K_4P_2O_7$ (0.1 M), prepared by dehydration of K_2HPO_4 at 600°C for 6 h. The pH of mixture of the resulting solution was controlled with hydrochloric acid HCl (0.5 M), afterwards it was left at room temperature, and crystals appeared within after 3 days.

2.2. X-ray crystallography

X-ray data were collected at 293 K on a colourless irregular block crystal of dimension $0.08 \times 0.21 \times 0.38\,mm^3$ using a Nonius Kappa CCD area detector diffractometer, with Mo$K\alpha$ radiation ($\lambda = 0.71070$ Å), in ϕ and ω scans mode. For unit-cell refinement 1055 reflections with $1.00° < \theta < 27.88°$ were used: the crystal is triclinic, space group $P\bar{1}$ ($Z = 2$), $a = 6.8565(2)$ Å, $b = 7.3621(3)$ Å, $c = 7.6202(3)$ Å, $\alpha = 81.044(2)°$, $\beta = 72.248(2)°$, $\gamma = 83.314(3)°$, $V = 360.90(2)$ Å^3, $D_c = 2.257\,g\,cm^{-3}$, $F(000) = 246$. 2415 reflections (1527 unique) were collected ($R_{int} = 0.033$), and omission of intensities with $I \leqslant 2\sigma(I_{obs})$ gave 1446 observed reflections employed for the analysis. Data were corrected for Lorentz and polarization effects. The structure was solved through the direct method procedure of SIR97 [14] and refined by a full-matrix least-squares technique based on F^2, SHELXL-97 [15]. The final formula of the compound resulted $KMg_{0.5}H_2P_2O_7 \cdot H_2O$. The non-hydrogen atoms were refined with anisotropic thermal parameters. The hydrogen atoms were localized through difference-Fourier map and refined isotropically. The final cycle of least-squares refinement included 122 parameters (weighting scheme applied: $w^{-1} = [\sigma^2(F_o^2) + (0.0422P)^2 + 0.2707P]$, with $P = [(F_o^2 + 2F_c^2)/3]$). The final residuals were $R = 0.0368$ and $wR = 0.0975$ ($I > 2\sigma(I_{obs})$), while GOF was 1.107. Crystal data and structure refinement are reported in Table 1, while fractional atomic coordinates and equivalent isotropic parameters are reported in Table 2.[1]

2.3. FT-IR spectroscopy

The infrared measurements were performed by a FT-IR Biorad spectrometer with resolution of $2\,cm^{-1}$ in the spectral range 400–4000 cm^{-1}, adopting the KBr pellets technique (1 mg sample per 400 mg KBr).

2.4. Raman spectroscopy

Micro-Raman measurements were performed in back-scattering geometry at room temperature by using a Dilor XY triple spectrometer with a liquid nitrogen cooled charge coupled device (CCD) detector and an adapted Olympus microscope. The spectra were excited with an Ar^+ laser (514.5 nm, 3 mW) and focused onto a spot of 2 μm in diameter. The scattered light was not analyzed in polarization; spectral resolution was

Table 1
Crystal data and structure refinement for $KMg_{0.5}(H_2P_2O_7) \cdot H_2O$

Empirical formula	$H_4KMg_{0.5}O_8P_2$
Formula weight	$245.23\,g\,mol^{-1}$
Temperature	293(2) K
Wavelength	0.71069 Å
Crystal system	Triclinic
Space group	$P\bar{1}$ (n. 2)
Unit-cell dimensions	$a = 6.8565(2)$ Å
	$b = 7.3621(3)$ Å
	$c = 7.6202(3)$ Å
	$\alpha = 81.044(2)°$
	$\beta = 72.248(2)°$
	$\gamma = 83.314(3)°$
V	360.90(2) Å^3
Formula units per cell	2
Calculated density	$2.257\,g\,cm^{-3}$
μ	$1.227\,mm^{-1}$
$F(000)$	246
Crystal size	$0.38 \times 0.21 \times 0.08\,mm^3$
θ range for data collection	2.81–27.82°
Range in $h\,k\,l$	$0 \leqslant h \leqslant 8$, $-9 \leqslant k \leqslant 9$, $-9 \leqslant l \leqslant 9$
Reflections collected	2415
Reflections independent	1527 ($R_{int} = 0.033$)
Refinement method	Full-matrix least-squares on F^2
Data/restraints/parameters	1446/0/122
Goodness-of-fit on F^2	1.107
Final R indices [$I > 2\sigma(I)$]	$R = 0.0368$, $wR = 0.0975$
R indices (all data)	$R = 0.0388$, $wR = 0.0995$
Largest diff. peak and hole	0.558 and $-0.626\,e\,Å^{-3}$

Table 2
Atomic coordinates and equivalent isotropic displacement parameters for $KMg_{0.5}(H_2P_2O_7) \cdot H_2O$

Atom	x	y	z	U_{iso}[a]
K1	0.38726(9)	−0.23635(8)	0.20817(8)	0.0365(2)
Mg1	0	0	0	0.0168(2)
P1	−0.25198(7)	0.31296(7)	0.25806(7)	0.0172(2)
P2	0.17488(7)	0.22789(7)	0.25150(7)	0.0177(2)
O1	−0.2375(2)	0.1755(2)	0.1288(2)	0.0227(3)
O2	−0.4324(3)	0.2858(2)	0.4384(2)	0.0253(4)
O3	−0.2520(3)	0.5108(2)	0.1709(2)	0.0269(4)
O4	−0.0645(2)	0.2753(2)	0.3480(2)	0.0243(4)
O5	0.1991(2)	0.1063(2)	0.1057(2)	0.0221(3)
O6	0.2604(2)	0.1495(2)	0.4077(2)	0.0244(3)
O7	0.2666(3)	0.4160(2)	0.1609(2)	0.0273(4)
O8	0.0560(3)	0.2032(2)	−0.2321(2)	0.0269(4)
H2	−0.507(7)	0.249(7)	0.418(6)	0.073(15)
H7	0.248(6)	0.451(6)	0.041(6)	0.070(12)
H8a	0.119(5)	0.186(5)	−0.338(5)	0.040(9)
H8b	0.096(6)	0.296(5)	−0.216(5)	0.050(10)

[a] Equivalent isotropic U is defined as one-third of the trace of the orthogonalized U_{ij} tensor.

[1] Further details of the crystal structure investigation can be obtained from the Fachinformationszentrum Karlsruhe, 76344 Eggenstein-Leopoldshafen, Germany (fax: +49-7247-808-666; mailto: crysdata@fiz-karlsruhe.de) on quoting the depository number CSD-412869.

0.5 cm^{-1}; lines of neon lamp were used for frequency scale calibration.

3. Results and discussion

3.1. X-ray crystal structure

The crystal packing of the title compound consists of layers parallel to *ab* plane formed by MgO_6 octahedra sharing four vertices with PO_3OH tetrahedra (Fig. 1). These layers, joint by K^+ cations and strong hydrogen bonds, build up a three-dimensional infinite network. All the atoms occupy general position except Mg1 which is at special position (0,0,0) and has a site occupancy of 0.5. The $Mg(H_2P_2O_7)_2 \cdot 2H_2O$ moiety can be described as C_i group as a result of the Mg1 central atom lying on the inversion center, with O(waters) atoms in *trans* position with respect to the P atoms plane (Fig. 2).

Mg1 atom forms a rather regular octahedron, with O8 water oxygen in apical positions. The distortion index, $[(\text{Cation–O})_{max}–(\text{Cation–O})_{min}]/\langle \text{Cation–O} \rangle$ [16], is 0.023: such low value is typical of Mg octahedra [13,17], basically due to the short Mg^{2+} ionic radius (0.72 Å). K atoms are involved in a complex coordination within cavities between P-tetrahedra and Mg-octahedra. According to Dumas et al. [6], which consider the K–O threshold bond of 3.19 Å, K1 atom forms an irregular octahedron (distortion index is 0.080), with K–O contact distances ranging from 2.768 up to 2.999 Å. By the analysis of polyhedra formed by

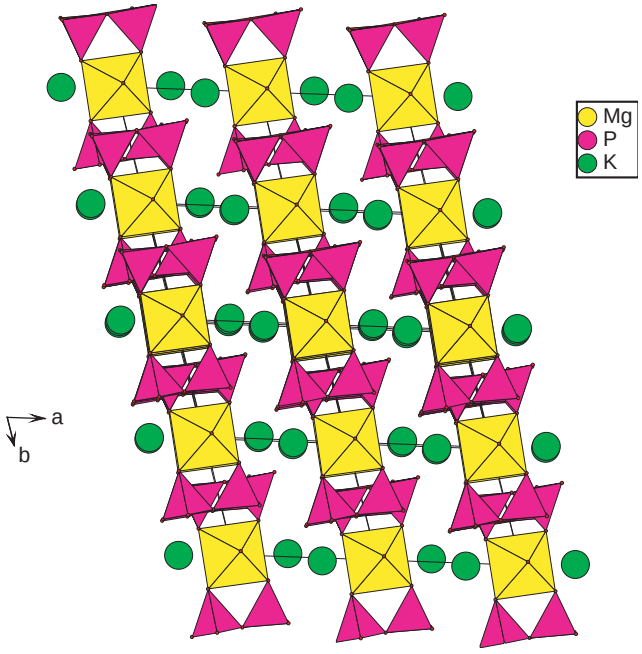

Fig. 1. Polyhedra representation of $KMg_{0.5}H_2P_2O_7 \cdot H_2O$ on the *ab* plane (supercell $2 \times 4 \times 2$): K–O bonds are omitted for clarity.

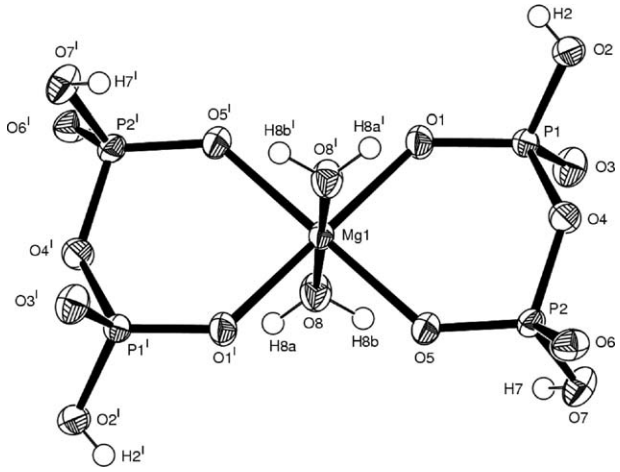

Fig. 2. $Mg(H_2P_2O_7)_2 \cdot 2H_2O$ group. Ellipsoids are drawn at 50% probability level. Symmetry code: $I: -x, -y, -z$.

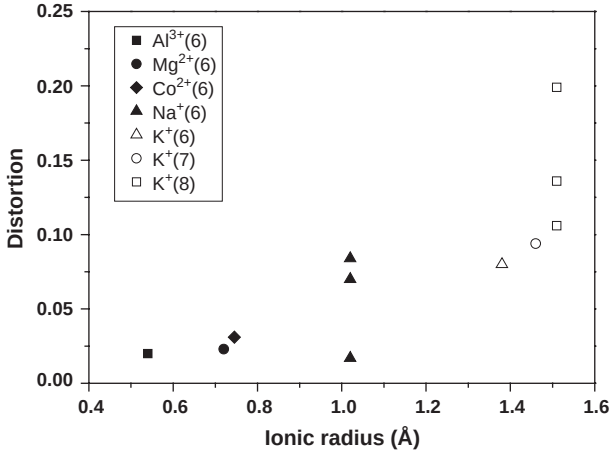

Fig. 3. Distortion index trend of coordination polyhedra [16] within inorganic dicationic dihydro-pyrophosphates [10–13]. Cation coordination number in parenthesis.

other cations in similar compounds, we can observe that the distortion increases with the ionic radius, being 0.020 for Al^{3+} octahedra (i.r. = 0.54 Å) [10], 0.031 for Co^{2+} octahedra (i. r. of 0.75 Å) [12], 0.017, 0.070 and 0.084 for Na^+ octahedra (i. r. of 1.02 Å) [11,13]; the lowest value for Na^+ octahedra (0.017) is related to the absence of water molecules in the compound $K_3Na(H_2P_2O_7)_2$, which allows a more compact crystal packing. Last, K^+ cation, because of its large dimensions (i.r. of 1.38, 1.46 and 1.51 Å for coordination numbers, respectively, 6, 7 and 8), forms more complex polyhedra, with distortion indexes extremely variable, ranging from 0.080 up to 0.199 [10–12]. The distortion index trend of coordination polyhedra within inorganic dicationic dihydro-pyrophosphates is depicted in Fig. 3 (ionic radii values from Ref. [18]). The P–O distances within PO_4 tetrahedra of $H_2P_2O_7$ group are comparable to those observed in dihydrogen pyrophosphate anions from

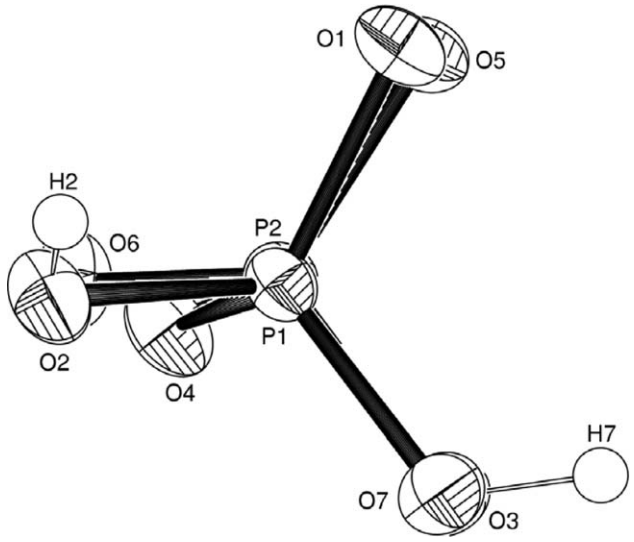

Fig. 4. Projection along the P1–P2 vector of $(H_2P_2O_7)^{2-}$ dianion showing its bent eclipsed conformation. Ellipsoids are drawn at 50% probability level.

Table 3
Selected bond lengths (Å) and angles (deg)

Bonds		Angles	
K1–O2^{I}	2.768(2)	P1–O4–P2	129.67(10)
K1–O5	2.807(2)		
K1–O7^{II}	2.886(2)	O1–P1–O3	114.78(9)
K1–O3^{III}	2.886(2)	O1–P1–O2	112.99(9)
K1–O8^{IV}	2.972(2)	O3–P1–O2	110.94(10)
K1–O1^{IV}	2.999(2)	O1–P1–O4	110.73(8)
		O3–P1–O4	107.24(9)
P1–O1	1.494(2)	O2–P1–O4	98.87(9)
P1–O3	1.504(2)	O6–P2–O5	116.27(9)
P1–O2	1.547(2)	O6–P2–O7	109.48(9)
P1–O4	1.610(2)	O5–P2–O7	110.09(9)
P2–O6	1.492(2)	O6–P2–O4	105.03(9)
P2–O5	1.492(2)	O5–P2–O4	109.37(8)
P2–O7	1.559(2)	O7–P2–O4	106.00(9)
P2–O4	1.602(2)		
Mg1–O1^{IV}	2.053(1)		
Mg1–O1	2.053(1)		
Mg1–O5^{IV}	2.059(1)		
Mg1–O5	2.059(1)		
Mg1–O8	2.100(2)		
Mg1–O8^{IV}	2.100(2)		

Simmetry code: I: $-x$, $-y$, $1-z$; II: x, $y-1$, z; III: $x+1$, $y-1$, z; IV: $-x$, $-y$, $-z$; V: $-x$, $-y$, $1-z$.

other structures [2,5,13]. It is possible to distinguish three types of P–O distances: P–O_b bonds (mean 1.606 Å), corresponding to the bridge oxygen, which are the longest ones, P–OH bonds (average 1.553 Å), involving hydroxyl groups, and P–O_{ext} corresponding to the external O atoms, which are the shortest ones (average 1.496 Å). The pyrophosphate anion shows bent eclipsed conformation (Fig. 4) with P1–O4–P2 angle 129.7(1)°. In Table 3 some selected bond lengths and angles are reported.

The shortest hydrogen bonds (Table 4) [O2⋯O6 = 2.522(3) and O7⋯O3 = 2.532(3) Å] correspond to strong interactions between hydroxyl groups and negative charged oxygens of $(H_2P_2O_7)^{2-}$ anion. These H-bonds belong to the [O–H⋯O]$^{-}$ class of negative-charge assisted H-bonds [(−)CAHB] [19–20] that, when perfectly symmetric, can become very strong with d(O⋯O) values down to 2.40 Å. Accordingly, the other hydrogen bonds donated by water molecules to the same oxygens are weaker and display longer distances [O8⋯O3 = 2.794(3) and O8⋯O6 = 2.742(2) Å].

3.2. Vibrational spectroscopy

The interpretation of Raman and infrared spectra (Figs. 5 and 6) can be made on the basis of characteristic vibrations of PO_2 group, P–OH bond, POP bridge and H_2O [13,21]. Band assignments for the fundamental modes of the compound are shown in Table 5. Broad bands in the region of stretching vibrations of water molecules (2500–3800 cm^{-1}) show the presence of a hydrogen bonding network. The splitting of the stretching and bending vibrations of water molecules respectively in the ranges 1600–1750 and 2500–3800 cm^{-1}, in both Raman and infrared spectra, is due to different hydrogen bond strengths and correlation field effect [22]. The frequencies of υOH are localized in both Raman and infrared spectra in the range 2300–3000 cm^{-1}. Bending δOH are located at 1278 and 1332 cm^{-1} in Raman, while the same vibrations are observed at 1262, 1290, 1333 and 1358 cm^{-1} in infrared spectrum.

The most intense band observed in the Raman spectrum at 1048 cm^{-1} is attributed to the symmetric terminal P–O stretching vibration of the PO_2 group. In

Table 4
Hydrogen bonding scheme: distances (Å) and angles (deg)

D–H		D⋯A		H⋯A		D–H⋯A	
O2–H2	0.67(6)	O2⋯O6^{I}	2.522(3)	H2⋯O6^{I}	1.86(5)	O2–H2⋯O6^{I}	170(6)
O7–H7	0.96(5)	O7⋯O3^{II}	2.532(3)	H7⋯O3^{II}	1.59(5)	O7–H7⋯O3^{II}	171(4)
O8–H8b	0.80(4)	O8⋯O3^{II}	2.794(3)	H8b⋯O3^{II}	2.00(5)	O8–H8b⋯O3^{II}	167(4)
O8–H8a	0.81(4)	O8⋯O6^{III}	2.742(2)	H8a⋯O6^{III}	1.93(4)	O8–H8a⋯O6^{III}	178(4)

Symmetry code: I: $x-1$, $+y$, $+z$; II: $-x$, $-y+1$, $-z$; III: x, $+y$, $+z-1$.

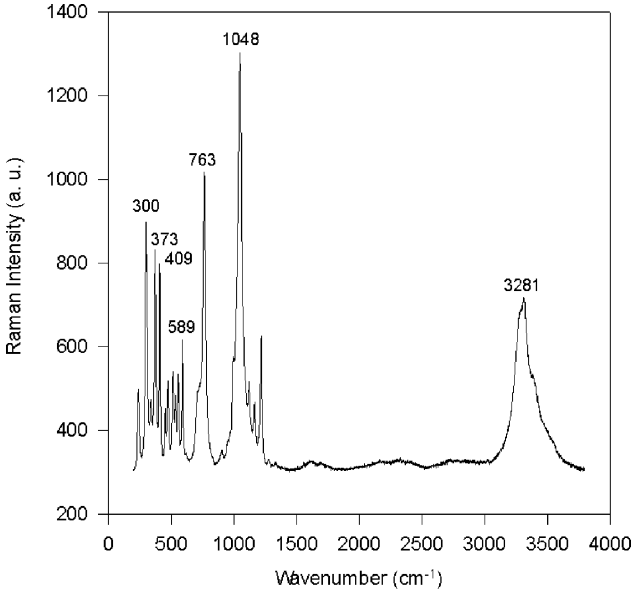

Fig. 5. Raman spectrum of $KMg_{0.5}H_2P_2O_7 \cdot H_2O$.

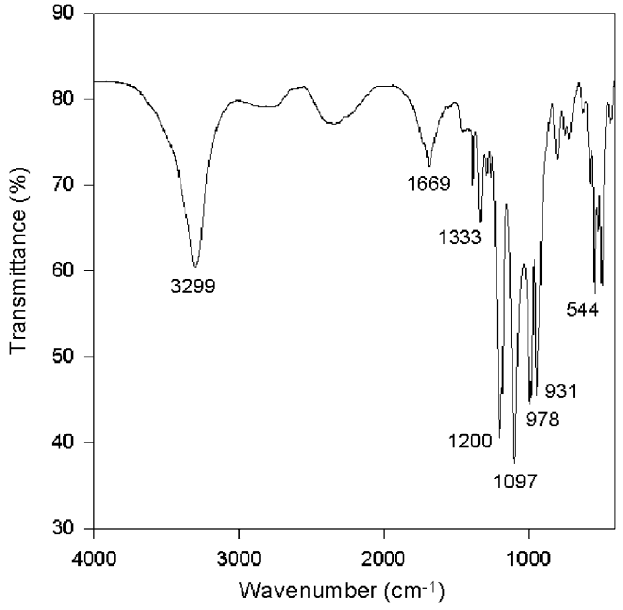

Fig. 6. Infrared spectrum of $KMg_{0.5}H_2P_2O_7 \cdot H_2O$.

Table 5
Band assignments for $KMg_{0.5}H_2P_2O_7 \cdot H_2O$

RA frequency (cm^{-1})	IR frequency (cm^{-1})	Assignments
3484vwb		
3387mb	3498wb	υH_2O
3318mb	3389wb	
3281sb	3299mb	
2787vwb	2858wb	υOH
2405vwb	2383wb	
2176vwb	2201wb	
1706vwb	1687w	
1605vwb	1669wb	δH_2O
1332vw	1385w	
1278vw	1333mb	δOH
	1290w	
	1262w	
1217s		
1165m	1200s	
1121m	1179s	$\upsilon_{as}PO_2$
1115vw	1097vs	
1080m		+
1048vs	1033mb	
1023m	1002w	υ_sPO_2
992m	994m	
955vw	978s	
900vw	946m	$\upsilon_{as}POP$
	931s	
	802w	
	751w	
763s	717w	υP–OH
729w		
		υ_sPOP
589s	622w	
555m	577w	ρH_2O
534m	544s	+
512m	520m	δPO_2
472m		+
452m	491s	ρPO_2
409s	431w	
381m		
373s		
365m		δPOP
339m		+
311m		Torsional modes
300s		+
245w		External modes

s = strong, m = medium, w = weak, v = very, b = broad, υ = stretching, δ = bending, ρ = rocking.

the infrared spectrum, the most intense band observed at $1097\,cm^{-1}$ is due to the asymmetric terminal stretching vibration of PO_2 group. For the behavior of the POP bridge vibrations, five components are observed in Raman spectrum, $\upsilon_{as}POP = 900$ and $955\,cm^{-1}$, $\upsilon_sPOP = 708$, 729 and $763\,cm^{-1}$, and five others in infrared spectrum at: $\upsilon_{as}POP = 931$, 946 and $978\,cm^{-1}$, $\upsilon_sPOP = 717$ and $751\,cm^{-1}$, which confirm the low symmetry of the cell [23]. The band located at $802\,cm^{-1}$ in infrared spectrum is due to the υP–OH mode [21].

The presence of υ_sPOP in infrared spectrum and $\upsilon_{as}POP$ in Raman spectrum leads to a bent POP bridge angle [23]. The δPO_2 and δP–OH are observed in the 350–600 cm^{-1} region [21]. In the Raman spectrum, the modes lying between 230–350 cm^{-1} can be attributed to the external, torsional and POP deformation modes, the

δPOP is observed at 300 cm^{-1} [24] and the rocking and the PO_2 deformation modes are observed in the 300–600 cm^{-1} region [21].

A comparison of the Raman and infrared bands shows that most of them are not coincident, which confirms a centrosymmetric structure of $KMg_{0.5}H_2P_2O_7 \cdot H_2O$.

References

[1] O.I. Andreeva, E.V. Efimtseva, N.S. Padyukova, S.N. Kochetkov, S.N. Mikhailov, H.B.F. Dixon, M.Y. Karpeisky, Mol. Biol. 35 (2001) 717–729.

[2] M. Mathew, L.W. Schroeder, W.E. Brown, J. Crystallogr. Spectrosc. Res. 23 (1993) 657–661.

[3] K. Byrappa, B.V. Umesh Dutt, A. Clearfield, M. Damodara Pojari, J. Mater. Res. 9 (1994) 1519–1525.

[4] D.E.C. Corbridge, Acta Crystallogr. 10 (1957) 85.

[5] R.L. Collin, M. Willis, Acta Crystallogr. B 27 (1971) 291–302.

[6] Y. Dumas, J.L. Galigne, J. Falgueirettes, Acta Crystallogr. B 29 (1973) 1623–1630.

[7] A. Durif, Crystal Chemistry of Condensed Phosphates, Plenum Publishing Corporation, New York, 1995.

[8] L.S. Ivashkevich, K.A. Selevich, A.S. Lyakhov, A.F. Selevich, Y.I. Petrusevich, Z. Kristallogr. 217 (2002) 73–77.

[9] H. Assaaoudi, A. Ennaciri, M. Harcharras, B. El Bali, F. Reinauer, R. Glaum, A. Rulmont, M.-R. Spirlet, Acta Crystallogr. C 58 (2002) i79–i81.

[10] O.V. Yakubovich, M.S. Dadashov, B.N. Litvin, Soviet physics, Crystallography 33 (1988) 16–19.

[11] Y. Dumas, J. Lapasset, J. Vicat, Acta Crystallogr. B 36 (1980) 2754–2757.

[12] A.A. Tahiri, R. Oursanal, M. Lachnar, B. El Bali, M. Bolte, Acta Crystallogr. E 58 (2002) i91–i92.

[13] M. Harcharras, H. Assaaoudi, A. Ennaciri, G. Mattei, V. D'Orazio, A.G.G. Moliterni, F. Capitelli, J. Solid State Chem. 172 (2003) 160–165.

[14] A. Altomare, M.C. Burla, M. Camalli, G.L. Cascarano, C. Giacovazzo, A. Guagliardi, A.G.G. Moliterni, G. Polidori, R. Spagna, J. Appl. Crystallogr. 32 (1999) 115–119.

[15] G.M. Sheldrick, SHELXL-97. Program for the Refinement of Crystal Structures, University of Gottingen, Germany, 1997.

[16] D. Kobashi, S. Kohara, J. Yamakawa, A. Kawahara, Acta Crystallogr. C 53 (1997) 1523–1525.

[17] M. Souhassau, C. Lecomte, R.H. Blessing, Acta Crystallogr. B 48 (1992) 370–376.

[18] R.D. Shannon, Acta Crystallogr. A 32 (1976) 751–767.

[19] P. Gilli, V. Bertolasi, V. Ferretti, G. Gilli, J. Am. Chem. Soc. 116 (1994) 909–915.

[20] V. Bertolasi, L. Pretto, P. Gilli, V. Ferretti, G. Gilli, New. J. Chem. 26 (2002) 1559–1566.

[21] O. Sarr, L. Diop, Spectrochim. Acta A 43 (1987) 999–1005.

[22] D.B. Philip, B. Lizbeth, G. Aruldhas, J. Raman Spectrosc. 21 (1990) 523–524.

[23] M. Harcharras, A. Ennaciri, A. Rulmont, B. Gilbert, Spectrochim. Acta A 53 (1997) 345–352.

[24] N. Santha, V.U. Nayar, G. Keresztury, Spectrochim. Acta A 49 (1993) 47–52.